ACS Catalysis

Research Article

pubs.acs.org/acscatalysis

Effect of Surface Oxygen on the Activation of Methane on Palladium and Platinum Surfaces

Xuefei Weng, Hongjia Ren, Mingshu Chen,* and Huilin Wan

State Key Laboratory of Physical Chemistry of Solid Surfaces, National Engineering Laboratory for Green Chemical Productions of Alcohols−Ethers−Esters, Department of Chemistry, College of Chemistry and Chemical Engineering, Xiamen University, Xiamen 361005, Fujian, China

ABSTRACT: Active surfaces for the catalytic oxidation of CH_4 on Pd and Pt were identified using infrared reflection absorption spectroscopy (IRAS) with a wide spectrum range (4000−450 cm^{-1}) that is capable of measuring both the surface species and changes specific to the surface. Both the metallic Pd and Pt surfaces were found to be significantly less active for the oxidation of CH_4 than the PdO surface under near-stoichiometric conditions. However, the metallic surfaces become very active under oxygen-poor conditions. This work represents the first evidence of such high activity for CH_4 oxidation on metallic Pt-group metal surfaces. A comparison of the catalytic behaviors of CH_4 and CO oxidation demonstrates that the chemisorbed oxygen with near-saturated coverage suppresses the activation of CH_4; additionally, the involvement of an unoccupied surface site, surface cation, or metallic atom can significantly enhance the activity for the activation of CH_4. The current results also demonstrate that oxygen is depleted sharply when switching from the combustion to the reforming region in the partial oxidation of methane to syngas.

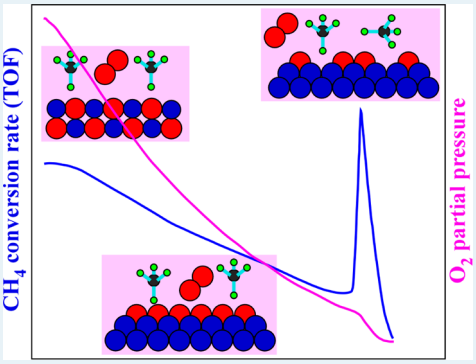

KEYWORDS: *methane oxidation, palladium, platinum, active surface, IRAS*

1. INTRODUCTION

Methane is a clean, low-carbon, and high-efficiency energy source and is abundantly found in natural gas, coal bed gas, shale gas, and CH_4 clathrates.[1−7] Methane is also a potential greenhouse gas, where catalytic oxidation can be used to reduce emissions of CH_4.[8−12] The relative abundance of CH_4 makes it an attractive alternative to oil. The direct conversion of methane to more-valuable chemicals, such as its selective oxidation to methanol and formaldehyde, oxidative coupling to ethylene, and aromatic dehydrogenation to benzene, has been thwarted by the low selectivity, activity, and stability of existing catalysts.[1−3,13−22] The partial oxidation of CH_4 (POM) to synthetic gas (syngas, CO + H_2), followed by Fischer−Tropsch chemistry,[1−3,13,14] has become a potential process for the development of liquefied alcohols, synthetic fuels, and light alkenes (key chemicals in industry). Although the partial oxidation of CH_4,[1−3,13,14,20−24] as well as the activation of CH_4,[25−41] has been extensively studied in recent years, the active surfaces and the mechanism leading to the formation of CO and H_2, by either a direct or combustion-reforming pathway, have not been fully clarified. The oxidation of CO and H_2 progresses rapidly on Pd-, Rh-, and Pt-based catalysts,[42−48] and the direct POM products may follow from subsequent oxidation to CO_2 and H_2O in the front part of the catalyst bed under O_2-rich conditions, resulting in the appearance of complete combustion. In such a case, the rear part of the catalyst bed suffers from O_2 deficiency; as a result, the CH_4 reforms CO_2 and H_2O to reproduce CO and H_2. The relative contribution of each process is difficult to identify, because the products are similar. Moreover, because the oxidation of CH_4 is a highly exothermic reaction, temperature gradients and reactant gradients are typically encountered during the catalytic partial oxidation of CH_4.[49−51] In most cases, a hot spot of several hundred Kelvin arises, and the reaction conditions change from oxidizing to reducing, which can also affect the nature of the active sites.[49−51] The complexity of this process, along with the support and additive effects, results in controversial knowledge regarding the nature of the catalytically active sites and the catalytic reaction mechanism for the oxidation of CH_4.[1−3,13,14,20−22,49−55]

Because of the significantly faster progression of the oxidation of CH_4 on Pt-group metals, compared to those for reforming, only a few percent of the packed catalyst is sufficient to fulfill the combustion reaction.[28,49,51−53] Moreover, a very sharp reactant gradient occurs in the front part of the catalyst bed for POM.[51−53,56,57] Because such high inhomogeneity is encountered in POM on the high-surface-area supported catalysts, it is difficult to elucidate a reliable structure−activity relationship. Recently, Chin et al. performed detailed experiments combined with a theoretical approach, offering significant insight into the reaction mechanism for POM.[29,34,42,43] Our previous *in situ* spectroscopic character-

Received: April 17, 2014
Revised: June 26, 2014
Published: June 27, 2014

izations and kinetic measurements confirmed that combustion-reforming is the main process by which the formation of syngas occurs, while direct partial oxidation is also possible for very short contact times (e.g., an extremely thin catalyst bed).[20−22] It was also found that the catalysts of supported Rh, Pd, and Pt were in the fully oxidized state as observed by *in situ* Raman spectroscopy before the ignition of POM, but turned to be a metallic state upon ignition.[20−22] However, it is still not known whether an oxidized region exists at the very front of the catalyst bed with metal-oxide amounts that are below the detection limit of *in situ* Raman spectroscopy.

In this study, resistively heated polycrystalline Pd and Pt thin foils served as model catalysts for the oxidation of CH_4, similar to the experimental setup in several previous reports.[56,58−62] We emphasize that the surface temperature was measured directly by a thermocouple attached to the metal foil; additionally, the studied surface was under the same reaction atmosphere at each moment, allowing our setup to overcome the hot spot and reactant gradient problems encountered in the combustion and partial oxidation of CH_4. The reaction products were mainly found to be CO_2 and H_2O using an online gas chromatograph, and the reaction rate was measured continuously by monitoring the total pressure change in a batch reactor, which is similar to the results in our previous study of CO oxidation on Pd.[46] Such experiments, in which the oxygen pressure decreases from its initial value to depletion, imitate the processes that occur in the front part of the catalyst bed, where the O_2 partial pressure decreases from the initial value to complete depletion under realistic POM reaction conditions. Moreover, *in situ* infrared reflection absorption spectroscopy (IRAS) with a wide spectrum range (4000−450 cm^{-1}), which covers the stretching vibrations for most oxides, was combined to collect surface information under these realistic catalytic reaction conditions.[48] Furthermore, reactions under conditions of excess CH_4 were examined. The most active surfaces for the catalytic oxidation of CH_4 over Pd and Pt were successfully identified. PdO was found to be significantly more active than both the metallic Pd and Pt under near-stoichiometric reaction conditions. However, the most active regions were found to be the metallic Pd and Pt surfaces under oxygen-poor conditions, where the surfaces were not saturated by chemisorbed oxygen. The oxidation of CO on the Pd surface, which is a well-documented catalytic reaction, was compared to obtain a better understanding of the observed phenomenon for the oxidation of CH_4.

2. EXPERIMENTAL SECTION

Experiments were carried out in a batch reactor (0.5 L) connected to a vacuum system and equipped with basic surface science techniques, including an ion gun for surface cleaning using Ar^+ sputtering, low-energy electron diffraction (LEED), and Auger electron spectroscopy (AES). The reactor was also furnished with *in situ* infrared reflection absorption spectrometry (IRAS) and online Agilent gas chromatography (GC) techniques, as well as a MKS precise pressure sensor. Details concerning the system used for our model catalysis study are provided in our previous publications.[48,63] The *in situ* reactor can accommodate a pressure range of ultrahigh vacuum (UHV) to 1 atm and sample temperatures of 80−1200 K. The wide spectrum range of *in situ* IRAS allows for the measurement of surface oxide formation and reduction and can be used to establish an authentic relationship between the surface structure and its catalytic activity.

The Pd and Pt thin foils measured 0.1 mm in thickness (Alfa Aesar) and were cleaned by chemical treatment before introduction into the vacuum chamber. The samples were heated resistively, while their temperatures were measured using a C-type thermocouple (5%Re/95%W−26%Re/74%W). Prior to the reaction, the samples were further cleaned and oxidized with O_2 at 600 K for 5 min and then were annealed under UHV at 900−1000 K to remove the residual oxygen. Average surface atom densities of 1.53×10^{15} and 1.47×10^{15} atoms/cm^2 for Pd and Pt, respectively, were used to estimate the turnover rate.

The possible products of the catalytic oxidation of CH_4 on Pd and Pt, respectively, are CO_2 and H_2O (complete oxidation) and CO and H_2 (partial oxidation). When crosschecked with an online Agilent gas chromatograph,[63] the main products were confirmed as CO_2 and H_2O (>99.9%) under the reaction conditions examined in this study. This is consistent with the general kinetics results of POM, namely, that feeding sufficient oxygen (CH_4:O_2 = 1:2) yields complete combustion products.[1−3,13,14] In addition, the oxidation of either CO or H_2 on both Pd and Pt occurs at significantly faster rates than that of CH_4.[28,29,42,45−48] The saturation pressures of CO_2 and H_2O are both below 10^{-6} Torr at the temperature of liquid nitrogen (78 K), while those of CH_4, O_2, and CO are ∼10.2, 160, and 360 Torr, respectively; in contrast, H_2 is not condensable at this temperature. Therefore, when using a liquid nitrogen trap with initial pressures of CH_4 and O_2 that are less than 10 and 160 Torr, respectively, the CO_2 and H_2O formed during the reaction will predominantly be trapped, while CO and H_2 will not be trapped. Therefore, the CH_4 oxidation rate ($CH_4 + 2O_2 = CO_2\downarrow + 2H_2O\downarrow$) can be continually monitored and computed from the decrease in total pressure. Partial oxidation, $CH_4 + {}^1/_2O_2 = CO + 2H_2$, will result in an increase in the total pressure. Hence, a decrease of the total pressure is correlated with the consumption of CH_4 and O_2.

High-purity CH_4 and O_2 (Hong Kong Specialty Gases Co., Ltd.) were further cleaned in a liquid nitrogen trap before introduction into the reaction cell. The cell was filled with a CH_4:O_2 gas mixture at the desired ratio and specified pressure at room temperature. Then, approximately one-seventh of the reactor was immersed into the liquid nitrogen bath to further clean the reactant gases and to remove the majority of the combustion products of CO_2 and H_2O. The sample temperatures were then increased to the reaction temperature to initiate the kinetic measurements. In the present study, pressure changes were measured using a MKS precision pressure sensor. The surface changes occurring under the reaction conditions, in particular, the formation and reduction of surface oxides, were characterized by our home-built *in situ* IRAS. The polycrystalline Pd and Pt foils were cleaned by preoxidizing in oxygen followed by annealing at 1000 K in UHV for 10 min to completely remove any residual oxygen.[46−48,64] The obtained clean surfaces were used to collect the IRAS background spectrum.

3. RESULTS AND DISCUSSION

Figure 1 shows *in situ* IRAS spectra for the oxidation of CH_4 on a Pd foil at 643 K. Upon the exposure of the clean Pd foil to the reactant mixture (CH_4 and O_2 of 9 and 1 Torr, respectively), while heating to 643 K, the Pd surface was oxidized to form PdO, as indicated by the two IR peaks at ∼645 cm^{-1} and ∼600 cm^{-1}. The assignments of these IR peaks were addressed

dx.doi.org/10.1021/cs500510x | ACS Catal. 2014, 4, 2598−2604

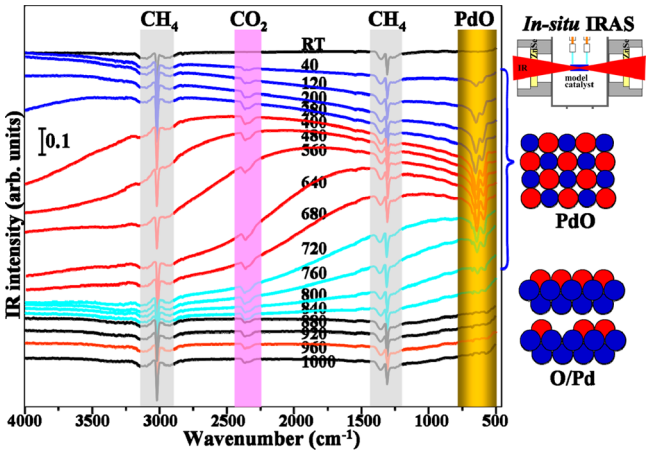

Figure 1. *In situ* IRAS spectra depict the formation and reduction of the Pd surface oxide during the oxidation of CH_4 at 643 K on a polycrystalline Pd thin foil. The bands of PdO as well as the gaseous phases of CH_4, CO_2, and H_2O are indicated in the figure. The initial CH_4 and O_2 pressures were 9 and 1 Torr in the batch reactor. The reaction times in seconds are labeled on the figure by corresponding spectra. The insets show the IRAS technique and cartoon-like surface structures of the PdO and chemisorbed oxygen covered surfaces (O/Pd).

previously in detail.[48] The formation of PdO was also confirmed by *in situ* Raman spectroscopy and was found to be consistent with the results presented in several previous approaches.[56,58−62,65−69] The ignition of the POM on Rh/Al_2O_3 was found to be potentially related to the amount of Rh present in the higher oxidation state;[51,67] this finding also sustains the interpretation that the oxide is an active surface. It should be noted that, because of the liquid nitrogen trap, the formation products of H_2O and CO_2 were held at very low levels in the gas phase, as can be observed in the *in situ* IR spectra (Figure 1).

The reaction kinetics were monitored based on changes in pressure, as shown in Figure 2A. The computed reaction rate in TOF (the turnover frequency, i.e., CH_4 molecules converted per surface Pd atom per second) is displayed in Figure 2B. The CH_4 conversion rate of the TOF was calculated based on the geometric Pd metal surface area, assuming an average Pd surface atom density of 1.53×10^{15} atoms cm^{-2}. The total pressure decreases rapidly at the beginning, concurrently accompanied by the appearance of PdO (Figures 1 and 2A). As the reaction proceeds, the O_2 partial pressure decreases quickly, while the CH_4 partial pressure remains at an almost constant level, because of the significant excess quantity (Figure 2A). The amount of PdO formed increases at the beginning, then is reduced at very low O_2 pressures (<0.2 Torr), in addition to an observed decrease in the reaction rate (Figure 2B). It should be noted that the as-formed PdO includes the bulk oxide, while the catalytic reaction takes place only on the surface; hence, the reaction rate need not follow the intensity of the PdO IR band. The observed decrease of the reaction rate as the O_2 pressure decreased and the amount of PdO is reduced leads to a complicated explanation, which may be related to the reaction order, with respect to O_2 pressure, as well as to the decrease of the effective active area of PdO. After ~890 s, the PdO peaks vanish, and the reaction rate reaches its lowest point (the TOF has decreased from 20 to 5). The CH_4 oxidation rate then increases on this reduced surface as the oxygen partial pressure further decreases. This sequence can be reproduced at

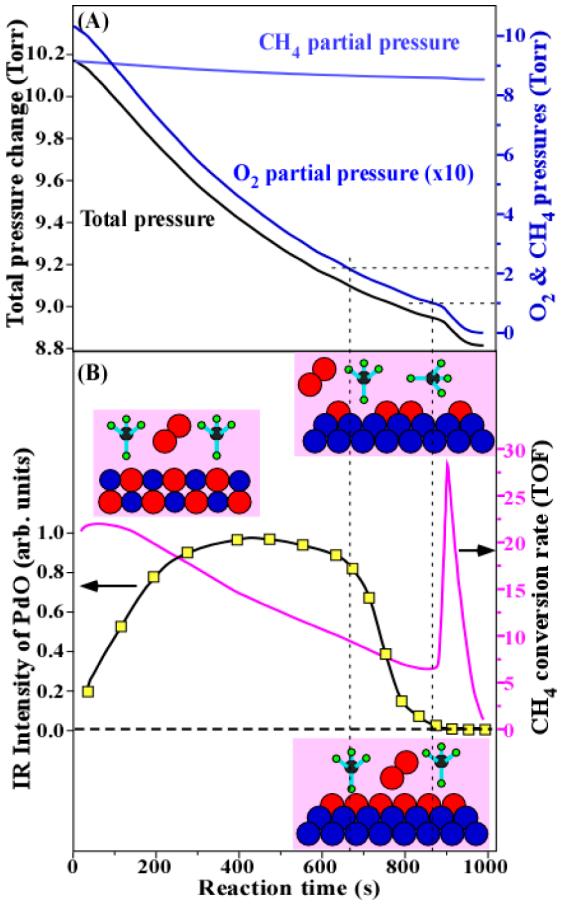

Figure 2. (A) The changes of the total pressure (black line) and partial pressure (blue line) are displayed, as functions of the reaction time, for a typical experiment of CH_4 oxidation on a polycrystalline Pd thin foil at 643 K. The initial CH_4 and O_2 pressures are 9 and 1 Torr, respectively. (B) The computed reaction rate (pink line) and IR intensity of PdO (black line) are displayed, as functions of the reaction time. The insets show cartoon-like surface structure models, according to the *in situ* IRAS results.

various reaction temperatures. The critical pressure ratio of O_2/CH_4 increases as the reaction temperature increases, as can be observed from the extent of the pressure drop from the critical point to the end of the reaction, as shown in Figure 3A.

For comparison, CH_4 oxidation was conducted on a polycrystalline Pt foil. With an initial CH_4/O_2 pressure ratio of 10/3, the CH_4 oxidation rate on Pt at 750 K was significantly lower than that on Pd at 643 K, although the rate increases continuously as the reaction proceeds, i.e., the O_2 partial pressure decreases (Figure 4A). The CH_4 conversion rate of TOF was calculated based on the geometric Pt metal surface area. The finding of a significantly lower rate for the oxidation of CH_4 on Pt, compared to Pd, was also reported previously.[56,59,70] Additionally, the ignition temperature for the oxidation of CH_4 on Pt/Al_2O_3 increased with an increase in oxygen concentration in the reactant mixture,[67] which also corroborates the suppression effect of oxygen. At a critical point of a CH_4/O_2 pressure ratio of ~20/1, the CH_4 reaction rate increases quickly and achieves a maximum that is ~2 orders of magnitude higher than the rate achieved under near-stoichiometric conditions. Such effect of O_2 pressure on the reaction rate for the oxidation of CH_4 was also observed on supported Pt catalysts, where a maximum TOF of ~1300 was

dx.doi.org/10.1021/cs500510x | ACS Catal. 2014, 4, 2598−2604

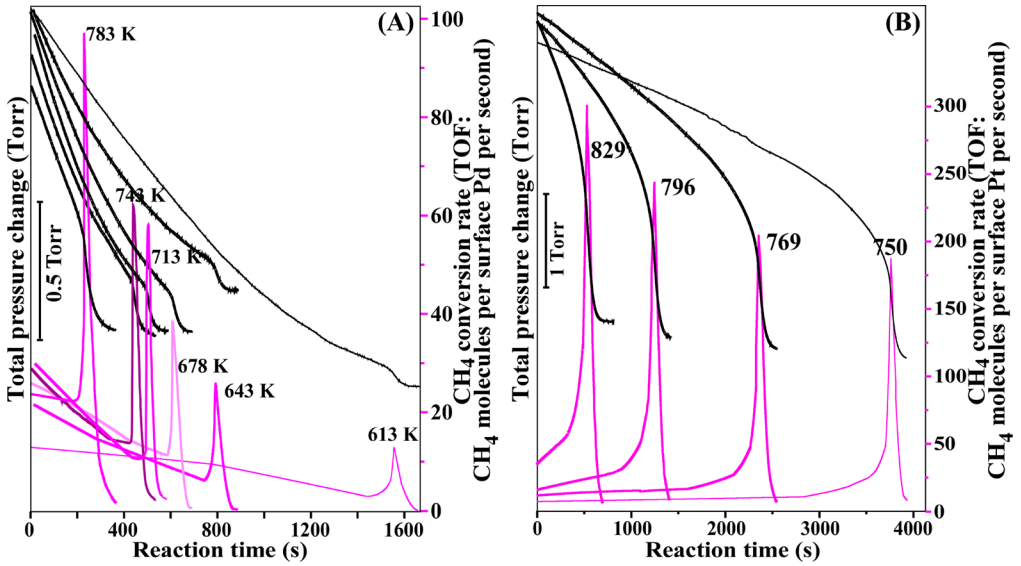

Figure 3. Changes in total pressure (black lines) and the computed reaction rates (pink lines), as functions of the reaction time for CH_4 oxidation over polycrystalline Pd and Pt thin foils at the indicated reaction temperatures: (A) over a Pd surface with an initial CH_4/O_2 ratio of 9/1 and a total pressure of 10 Torr and (B) over a Pt surface with an initial CH_4/O_2 ratio of 10/3 and a total pressure of 13 Torr.

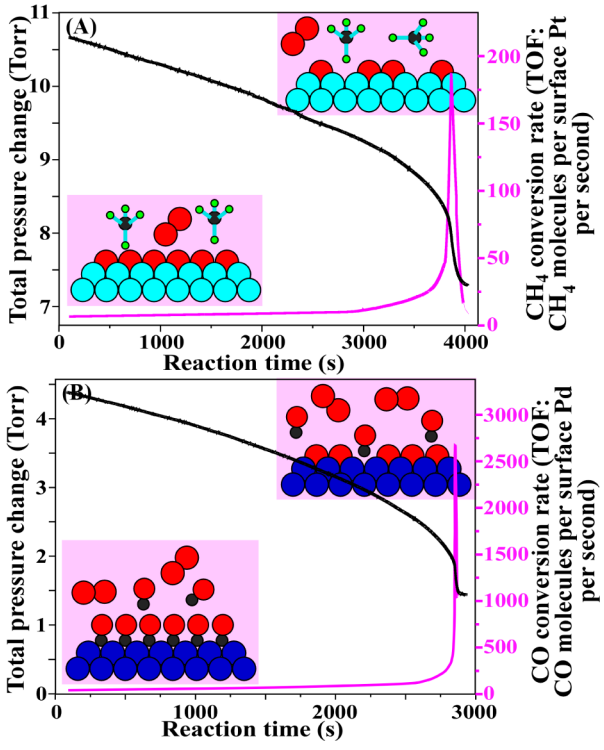

Figure 4. Changes of the total pressure (black line) and the computed reaction rates (pink line), as functions of the reaction time for (A) CH_4 oxidation over a polycrystalline Pt thin foil at 750 K with an initial CH_4/O_2 ratio of 10/3 and a total pressure of 13 Torr, and (B) CO oxidation over the polycrystalline Pd thin foil at 523 K with an initial CO/O_2 ratio of 1/1.2 and a total pressure of 5 Torr. The insets show cartoon-like surface structure models based on IRAS measurements.

achieved with an CH_4/O_2 pressure ratio of ~10/1 at 873 K.[42] We emphasize that the critical O_2/CH_4 pressure ratio increases with the reaction temperature, as shown in Figure 3B. Because platinum oxides were not detected (a band with a frequency of 500−700 cm^{-1} would be expected[71,72]) by *in situ* IRAS and Raman spectroscopies during the oxidation of CH_4 on the Pt thin foil, it is reasonable to conclude that metallic Pt is the active surface under the present conditions, consistent with a recent report.[42] Here, it should be noted that platinum oxide does form for oxide-supported Pt nanoparticles before the point of ignition under POM conditions, but reduces to the metallic state upon ignitation.[21,22] These results demonstrate that PdO is significantly more active for CH_4 oxidation than either metallic Pd or Pt under comparable reaction conditions. Previous kinetic measurements on Pd also yielded observations of a significant drop of the reaction rate upon the transformation of PdO to the metallic Pd phase as the reaction temperature increased to values above 950 K (1.5 Torr O_2 + 0.3 Torr CH_4).[56] A recent *in situ* surface X-ray diffraction study also confirmed PdO as one of the active surfaces for CH_4 oxidation.[66] The temperature-programmed desorption of light alkanes revealed that CH_4 molecules bond more strongly on PdO surfaces than on Pd surfaces due to the formation of a sigma-complex,[68] which may be one reason for the corresponding higher reaction rate.

The above results demonstrate that significantly higher reaction rates (Figures 2, 3 and 4), specifically, 2−3 orders of magnitude higher than those observed under near-stoichiometric conditions, are achieved on Pd and Pt surfaces under oxygen-poor conditions. Such high rates are even more remarkable when compared to those observed on PdO surfaces, especially at higher reaction temperatures (Figure 3). To better understand this phenomenon, CO oxidation was performed in the same reactor using the same Pd sample. It should be noted that such a sharp enhancement of the reaction rate, as a function of the CO partial pressure, has previously been observed for the oxidation of CO on Pd, Rh, and Pt metals.[46−48] As observed in Figure 4B, CO oxidation was conducted on the Pd thin foil at 523 K in the same reactor as that used for CH_4 oxidation. Beginning with an oxygen-rich condition, the extent of the total pressure decrease increases with reaction progress, i.e., the reaction rate increases as the CO partial pressure decreases (a negative order of 1.2 with respect to the CO pressure), see also Figure 5A. A very sharp pressure drop, corresponding to a TOF of 2000−3000 (2−3

dx.doi.org/10.1021/cs500510x | *ACS Catal.* 2014, 4, 2598−2604

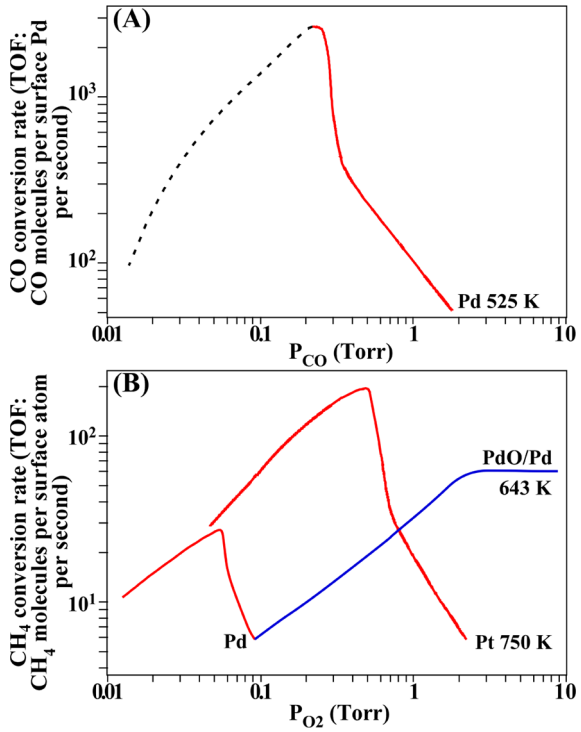

Figure 5. Reaction order dependence for (A) CO oxidation over a Pd foil at 523 K on CO (~0−3 Torr CO, 1.5−3 Torr O_2) and (B) CH_4 oxidation over a Pd foil at 643 K and over a Pt foil at 750 K on O_2 (~10 Torr CH_4, and 0−10 Torr O_2).

orders of magnitude higher than that observed under the near-stoichiometric condition), is observed at the critical CO/O_2 pressure ratio. It has been well-established that Pd and Pt surfaces are dominated by CO, even under oxygen-rich conditions during CO oxidation; this fact results in CO-desorption limiting of the reaction rate.[42−48,73] As the CO partial pressure decreases, the surface coverage of the chemisorbed CO decreases, vacating more surface sites for O_2 activation and leading to a very sharp growth of the reaction rate at low levels of surface oxygen coverage. Then, the reaction rate either achieves a maximum value at suitable surface coverages of CO and O or meets the mass transfer limit of CO, resulting in the shift from a CO-dominant surface to a chemisorbed oxygen-dominant surface.[48] It should be noted that *in situ* IRAS with a wide spectrum range has demonstrated that PdO does not appear for CO oxidation under the above-mentioned conditions.[48]

In contrast, the CH_4 conversion rates (TOF) on metallic Pd and Pt surfaces are low under the above-examined conditions, as shown in Figures 2, 4, and 5. However, the dissociation of O_2 on Pd and Pt surfaces is well-known to occur quickly,[74−77] which can also be substantiated from the oxidation of CO with a TOF of several hundreds to several thousands at lower reaction temperatures of 450−550 K (Figures 4 and 5).[46−48] The lower CH_4 reaction rate should then be limited by the activation of CH_4 on the Pt and Pd surfaces. Moreover, surface CH_x (x = 0−3) species were not observed by subtracting the *in situ* IRAS spectra obtained under the reaction conditions, when using the comparable gas phase CH_4 as a background. Based on these facts, the surfaces of Pd and Pt under the CH_4 oxidation conditions should be dominated by chemisorbed oxygen, if the specific oxides are not present.

Accordingly, the initial lower CH_4 conversion rate observed on the Pt surface and the increase of the reaction rate with decreasing O_2 partial pressure (a negative order of ~1.4, with respect to the O_2 pressure) demonstrate that the surface-chemisorbed oxygen at near-saturation coverage suppresses the activation of CH_4, i.e., CH_4 activation requires unoccupied Pt sites. This is also evidenced by the similarity of the trend lines of the changes in the total pressure and rate for the oxidation of CH_4 on Pt as functions of the reaction time, in addition to the trends recorded for the oxidation of CO on Pd and Pt (see Figure 5).[48] It has also been proposed that a surface that is unsaturated with chemisorbed oxygen (oxygen-vacancy pair: O*−*) is more active than a surface that is saturated with chemisorbed oxygen, based on kinetic measurements for the oxidation of CH_4 on supported Pt nanoparticles and DFT calculations.[28,34] Therefore, with decreasing in O_2 pressure, the coverage of the surface chemisorbed oxygen (θ_O) decreases, which then releases additional active sites on the surface (uncovered surface Pt atoms) for the activation of CH_4, leading to an increase in the reaction rate (a negative order of 1.4, with respect to O_2; see Figure 5B). As the critical point is approached, the number of available surface Pt sites increases significantly, resulting in a sharp increase in the reaction rate. This continues until a maximum reaction rate has been achieved. After the maximum point, the rate decreases with a further decrease of the O_2 pressure due to the presence of an insufficient amount of surface oxygen species.

Even at a CH_4/O_2 pressure ratio of 10/1, PdO initially forms on the Pd surface; hence, this system exhibits a higher reaction rate and changes by +0.9 orders with respect to the O_2 pressure (Figure 5). PdO is reduced at low O_2 partial pressures (Figures 1 and 2); after this occurs, the behavior of CH_4 oxidation on the metallic Pd at low O_2 pressure is similar to that on the Pt surface. There are common features between the two systems, including the increase in the reaction rates (TOFs) with decreasing CO partial pressure, with respect to CO oxidation, and with decreasing O_2, with respect to CH_4 oxidation, and the occurrence of a sharp increase at the critical point. It should be noted that de-N_2O efficiency on Pd/Al_2O_3 catalysts in the presence of CH_4 and O_2 is also significantly suppressed by O_2, due to the scavenging of strongly adsorbed oxygen species by the hydrocarbon.[78]

Furthermore, it should be emphasized that O_2 can dissociate on metallic Pd surfaces to form a chemisorbed oxygen species below room temperature,[74−76,79−82] while the formation of a bulk oxide requires a higher temperature and sufficient O_2 partial pressure.[48,83,84] The reduction of PdO as the O_2 partial pressure decreases under the CH_4 oxidation conditions demonstrates that the O_2 partial pressure is essential to PdO stability in the presence of a certain amount of the reducing gas.[84] Such results also suggest that the activation/dissociation of O_2 on the PdO surface is slower than that on the metallic Pd surface, as well as the fact that the lattice oxygen can directly engage in CH_4 oxidation.

The above comparisons demonstrate that strongly chemisorbed oxygen species are involved in the oxidation of both CH_4 and CO on Pd and Pt, when no oxide has formed. Under near-stoichiometric conditions, the surface is dominated by chemisorbed oxygen for the oxidation of CH_4, but chemisorbed CO dominates the surface for the oxidation of CO. The state of higher activity occurs under oxygen-poor conditions on a chemisorbed oxygen-deficient surface during CH_4 oxidation, but under oxygen-rich conditions on a chemisorbed oxygen-

dx.doi.org/10.1021/cs500510x | *ACS Catal.* 2014, 4, 2598−2604

rich surface during CO oxidation. These results reveal that the Pd and Pt surfaces are rich in surface chemisorbed oxygen for CH_4 oxidation, while such oxygen-rich surfaces are highly active for the oxidation of CO. This is the reason why CO_2 and H_2O are the main products during the oxidation of CH_4 on Pd and Pt under the present experimental conditions, except when O_2 is nearly depleted. This supports a mechanism of combustion followed by subsequent reforming for the partial oxidation of methane.[1−3,13,14] The very sharp pressure drop observed at the critical point also confirms the complete oxidation of CH_4 because partial oxidation ($CH_4 + 0.5O_2 = CO + 2H_2$), including both the direct and combustion-reforming paths, would result in a pressure increase.

The significantly different activities observed for the oxidation of CH_4 on Pd and Pt surfaces as a function of O_2 pressure (Figure 5) demonstrate that the combination of Pd and Pt on a supported catalyst should enhance the overall activity of the catalyst in a wide range of O_2 pressures in which PdO may play the key role under oxygen-rich conditions, while Pt may be the key catalytically active surfaces under oxygen-poor conditions. The better performance observed on a bimetallic Pd−Pt catalyst for the oxidation of CH_4[85] can be attributed partially to the effect of alloying, which modifies the redox properties of Pd nanoparticles, in addition to the existence of different active surfaces of PdO and metallic Pt.

4. CONCLUSIONS

In summary, both PdO and metallic Pd were identified by the home-built wide spectrum range *in situ* IRAS as catalytically active surfaces for the oxidation of CH_4, depending on the reaction temperature and the partial pressure of O_2. On a bulk-like Pt foil, only the metallic surface presents as the active surface. Near stoichiometric reaction conditions, the PdO surface is significantly more active for CH_4 oxidation than either the metallic Pd or Pt surfaces. The dissociated adsorption of O_2 occurs significantly faster than that of CH_4 on the Pd and Pt surfaces, leading to a surface dominated by chemisorbed oxygen on both the metallic Pd and Pt surfaces, which then suppresses the activation of CH_4. The most active region is achieved under oxygen-poor conditions. The study reveals that the involvement of a surface metal or cation site significantly enhances the activation rate of CH_4.

AUTHOR INFORMATION

Corresponding Author

*Tel./Fax: 86-592-2183723. E-mail: chenms@xmu.edu.cn.

Notes

The authors declare no competing financial interest.

ACKNOWLEDGMENTS

We gratefully acknowledge the support received by this work from the National Basic Research Program of China (973 program: No. 2013CB933102), the Major Project of the Chinese Ministry of Education (No. 309019), the National Natural Science Foundation of China (Nos. 21033006, 21073149, 21273178), the Program for Changjiang Scholars and Innovative Research Team in University (No. IRT1036), and the Ph.D. Programs Foundation of the Chinese Ministry of Education (No. 20110121110010). We thank Ying Lin and Ying Zeng for their excellent assistance during the *in situ* measurements.

REFERENCES

(1) Pena, M. A.; Gomez, J. P.; Fierro, J. L. G. *Appl. Catal., A* **1996**, *144*, 7−57.
(2) Lunsford, J. H. *Catal. Today* **2000**, *63*, 165−174.
(3) Hickman, D. A.; Schmidt, L. D. *Science* **1993**, *259*, 343−346.
(4) Murray, E. P.; Tsai, T.; Barnett, S. A. *Nature* **1999**, *400*, 649−651.
(5) Trimm, D. L.; Onsan, Z. I. *Catal. Rev.−Sci. Eng.* **2001**, *43*, 31−84.
(6) Park, S. D.; Vohs, J. M.; Gorte, R. J. *Nature* **2000**, *404*, 265−267.
(7) Boswell, R. *Science* **2009**, *325*, 957−958.
(8) Oh, S. E.; Mitchell, P. J.; Siewert, R. M. *J. Catal.* **1991**, *132*, 287−301.
(9) Ciuparu, D.; Lyubovsky, M. R.; Altman, E.; Pfefferle, L. D.; Datye, A. *Catal. Rev.−Sci. Eng.* **2002**, *44*, 593−649.
(10) Gelin, P.; Primet, M. *Appl. Catal., B* **2002**, *39*, 1−37.
(11) Cargnello, M.; Jaen, J. J. D.; Garrido, J. C. H.; Bakhmutsky, K.; Montini, T.; Gamez, J. J. C.; Gorte, R. J.; Fornasiero, P. *Science* **2012**, *337*, 713−717.
(12) Lu, Y.; Michalow, K. A.; Matam, S. K.; Winkler, A.; Maegli, A. E.; Yoon, S.; Heel, A.; Weidenkaff, A.; Ferri, D. *Appl. Catal., B* **2014**, *144*, 631−643.
(13) Enger, B. C.; Lødeng, R.; Holmen, A. *Appl. Catal., A* **2008**, *346*, 1−27.
(14) Branco, J. B.; Ferreira, A. C.; do Rego, A. M. B.; Ferraria, A. M.; Almeida-Gaschet, T. *ACS Catal.* **2012**, *2*, 2482−2489.
(15) Lee, J. S.; Oyama, S. T. *Catal. Rev.−Sci. Eng.* **1988**, *30*, 249−280.
(16) Wang, L. S.; Tao, L. X.; Xie, M. S.; Xu, G. F.; Huang, J. S.; Xu, Y. D. *Catal. Lett.* **1993**, *21*, 35−41.
(17) Periana, R. A.; Taube, D. J.; Gamble, S.; Taube, H.; Satoh, T.; Fujii, H. *Science* **1998**, *280*, 560−564.
(18) Otsuka, K.; Wang, Y. *Appl. Catal., A* **2001**, *222*, 145−161.
(19) Tomita, A.; Nakajima, J.; Hibino, T. *Angew. Chem., Int. Ed.* **2008**, *47*, 1462−1464.
(20) Wei, Z. W.; Ming, S. C.; Hui, L. W. *Chem. Rec.* **2002**, *2*, 102−112.
(21) Wang, M. L.; Zheng, H. Z.; Li, J. M.; Weng, W. Z.; Xia, W. S.; Huang, C. J.; Wan, H. L. *Chem.—Asian J.* **2011**, *6*, 580−589.
(22) Liu, Y.; Huang, F. Y.; Li, J. M.; Weng, W. Z.; Luo, C. R.; Wang, M. L.; Xia, W. S.; Huang, C. J.; Wan, H. L. *J. Catal.* **2008**, *256*, 192−203.
(23) Chalupka, K. A.; Jozwiak, W. K.; Rynkowski, J.; Maniukiewicz, W.; Casale, S.; Dzwigaj, S. *Appl. Catal., B* **2014**, *146*, 227−236.
(24) Cimino, S.; Mancino, G.; Lisi, L. *Appl. Catal., B* **2013**, *138*, 342−352.
(25) Jones, W. D. *Acc. Chem. Res.* **2003**, *36*, 140−146.
(26) Juurlink, L. B. F.; Killelea, D. R.; Utz, A. L. *Prog. Surf. Sci.* **2009**, *84*, 69−134.
(27) Schwarz, H. *Angew. Chem., Int. Ed.* **2011**, *50*, 10096−10115.
(28) Chin, Y. H.; Buda, C.; Neurock, M.; Iglesia, E. *J. Am. Chem. Soc.* **2011**, *133*, 15958−15978.
(29) Choudhary, T. V.; Aksoylu, E.; Goodman, D. W. *Catal. Rev.−Sci. Eng.* **2003**, *45*, 151−203.
(30) Luntz, A. C.; Bethune, D. S. *J. Chem. Phys.* **1989**, *90*, 1274−1280.
(31) Duarte, R. B.; Safonova, O. V.; Krumeich, F.; Makosch, M.; van Bokhoven, J. A. *ACS Catal.* **2013**, *3*, 1956−1964.
(32) Kondo, T.; Sasaki, T.; Yamamoto, S. *J. Chem. Phys.* **2003**, *118*, 760−767.
(33) Fuhrmann, T.; Kinne, M.; Whelan, C. M.; Zhu, J. F.; Denecke, R.; Steinruck, H. P. *Chem. Phys. Lett.* **2004**, *390*, 208−213.
(34) Wei, J. M.; Iglesia, E. *J. Phys. Chem. B* **2004**, *108*, 4094−4103.
(35) Tait, S. L.; Dohnalek, Z.; Campbell, C. T.; Kay, B. D. *Surf. Sci.* **2005**, *591*, 90−107.
(36) Marsh, A. L.; Becraft, K. A.; Somorjai, G. A. *J. Phys. Chem. B* **2005**, *109*, 13619−13622.
(37) Psofogiannakis, G.; St. Amant, A.; Ternan, M. *J. Phys. Chem. B* **2006**, *110*, 24593−24605.
(38) Cushing, G. W.; Navin, J. K.; Donald, S. B.; Valadez, L.; Johanek, V.; Harrison, I. *J. Phys. Chem. C* **2010**, *114*, 17222 (and Erratum, p 22790).

(39) Enterkin, J. A.; Setthapun, W.; Elam, J. W.; Christensen, S. T.; Rabuffetti, F. A.; Marks, L. D.; Stair, P. C.; Poeppelmeier, K. R.; Marchall, C. L. *ACS Catal.* **2011**, *1*, 629−635.
(40) Zhang, R. G.; Song, L. Z.; Wang, Y. H. *Appl. Surf. Sci.* **2012**, *258*, 7154−7160.
(41) Navin, J. K.; Donald, S. B.; Tinney, D. G.; Cushing, G. W.; Harrison, I. *J. Chem. Phys.* **2012**, *136*, 061101(−4).
(42) Chin, Y. H.; Buda, C.; Neurock, M.; Iglesia, E. *J. Catal.* **2011**, *283*, 10−24.
(43) Chin, Y. H.; Buda, C.; Neurock, M.; Iglesia, E. *J. Am. Chem. Soc.* **2011**, *133*, 15958−15978.
(44) Su, X. C.; Cremer, P. S.; Shen, Y. R.; Somorjai, G. A. *J. Am. Chem. Soc.* **1997**, *119*, 3994−4000.
(45) Ackermann, M. D.; Pedersen, T. M.; Hendriksen, B. L. M.; Robach, O.; Bobaru, S. C.; Popa, I.; Quiros, C.; Kim, H.; Hammer, B.; Ferrer, S.; Frenken, J. W. M. *Phys. Rev. Lett.* **2005**, *95*, 255505.
(46) Chen, M. S.; Cai, Y.; Yan, Z.; Gath, K. K.; Axnanda, S.; Goodman, G. W. *Surf. Sci.* **2007**, *601*, 5326−5331.
(47) Gao, F.; Goodman, D. W. *Langmuir* **2012**, *26*, 16540−16551.
(48) Chen, M. S.; Wang, X. V.; Zhang, L. H.; Tang, Z. Y.; Wan, H. L. *Langmuir* **2010**, *26*, 18113−18118.
(49) Boucouvalas, Y.; Zhang, Z. L.; Verykios, X. E. *Catal. Lett.* **1994**, *27*, 131−142.
(50) Dissanayake, D.; Rosynek, M. P.; Kharas, K. C. C.; Lunsford, J. H. *J. Phys. Chem.* **1993**, *97*, 36644−36646.
(51) Grunwaldt, J.-D.; Hannemann, S.; Schroer, C. G.; Baiker, A. *J. Phys. Chem. B* **2006**, *110*, 8674−8680.
(52) Donazzi, A.; Beretta, A.; Groppi, G.; Forzatti, P. *J. Catal.* **2008**, *255*, 241−258 & 259−268.
(53) Korup, O.; Goldsmith, C. F.; Weinberg, G.; Geske, M.; Kandemir, T.; Schlögl, R.; Horn, R. *J. Catal.* **2013**, *297*, 1−16.
(54) Campa, M. C.; Ferraris, G.; Gazzoli, D.; Pettiti, I.; Pietrogiacomi, D. *Appl. Catal., B* **2013**, *142*, 423−431.
(55) Meng, L.; Lin, J. J.; Pu, Z. Y.; Luo, L. F.; Jia, A. P.; Huang, W. X.; Luo, M. F.; Lu, J. Q. *Appl. Catal., B* **2013**, *119*, 117−122.
(56) Zhu, G. H.; Han, J. Y.; Zernlyanov, D. Y.; Ribeiro, F. H. *J. Phys. Chem. B* **2005**, *109*, 2331−2337.
(57) Rodrigues, M. T. S.; Silva, R. B.; Rocha, M. G. C.; Bargiela, P.; Noronha, F. B.; Brandao, S. T. *Catal. Today* **2012**, *197*, 137−143.
(58) Haack, L. P.; Otto, K. *Catal. Lett.* **1995**, *34*, 31−40.
(59) Aryafar, M.; Zaera, F. *Catal. Lett.* **1997**, *48*, 173−183.
(60) (a) Monteiro, R. S.; Zemlyanov, D.; Storey, J. M.; Ribeiro, F. H. *J. Catal.* **2001**, *199*, 291−301. (b) Monteiro, R. S.; Zemlyanov, D.; Storey, J. M.; Ribeiro, F. H. *J. Catal.* **2001**, *201*, 37−45.
(61) Xu, J.; Ouyang, L. K.; Mao, W.; Yang, X. J.; Xu, X. C.; Su, J. J.; Zhuang, T. Z.; Li, H.; Han, Y. F. *ACS Catal.* **2012**, *2*, 261−269.
(62) Han, J. Y.; Zemlyanov, D. Y.; Ribeiro, F. H. *Catal. Today* **2006**, *117*, 506−513.
(63) Zhen, Y. P.; Zhang, L. H.; Wang, S. L.; Ding, D.; Chen, M. S.; Wan, H. L. *Langmuir* **2013**, *29*, 9090−9097.
(64) Penner, S.; Bera, P.; Pedersen, S.; Ngo, L. T.; Harris, J. J. W.; Campbell, C. T. *J. Phys. Chem. B* **2006**, *110*, 24577−24584.
(65) Descorme, C.; Jacobs, P. W.; Somorjai, G. A. *J. Catal.* **1998**, *178*, 668−678.
(66) Hellman, A.; Resta, A.; Martin, N. M.; Gustafson, J.; Trinchero, A.; Carlsson, P. A.; Balmes, O.; Felici, R.; van Rijn, R.; Frenken, J. W. M.; Andersen, J. N.; Lundgren, E.; Gronbeck, H. *J. Phys. Chem. Lett.* **2012**, *3*, 678−682.
(67) (a) Bourane, A.; Cao, C.; Hohn, K. L. *Appl. Catal., A* **2006**, *302*, 224−231. (b) Bourane, A.; Cao, C.; Hohn, K. L. *Appl. Catal., A* **2008**, *344*, 78−87.
(68) Weaver, J. F.; Hakanoglu, C.; Hawkins, J. M.; Asthagiri, A. *J. Chem. Phys.* **2010**, *132*, 024709 (−10).
(69) Munoz, F. F.; Baker, R. T.; Leyva, A. G.; Fuentes, R. O. *Appl. Catal., B* **2013**, *136*, 122−132.
(70) Fang, Y.; Yao, Y. *Ind. Eng. Chem. Prod. Res. Dev.* **1980**, *19*, 293−298.
(71) Graham, G. W.; Weber, W. H.; McBride, J. R.; Peters, C. R. *J. Raman Spectrosc.* **1991**, *22*, 1−9.
(72) Chan, H. Y. H.; Zou, S.; Weaver, M. J. *J. Phys. Chem. B* **1999**, *103*, 11141−11151.
(73) Satsuma, A.; Osaki, K.; Yanagihara, M.; Ohyama, J.; Shimizu, K. *Appl. Catal., B* **2013**, *132*, 511−518.
(74) Engel, T.; Ertl, G. A. *J. Phys. Chem.* **1978**, *69*, 1267−1281.
(75) Berlowitz, P. J.; Peden, C. H. F.; Goodman, D. W. *J. Phys. Chem.* **1988**, *92*, 5213−5221.
(76) Liu, J.; Xu, M.; Zaera, F. *Catal. Lett.* **1996**, *37*, 9−13.
(77) Getman, R. B.; Schneider, W. F.; Smeltz, A. D.; Delgass, W. N.; Ribeiro, F. H. *Phys. Rev. Lett.* **2009**, *102*, 076101.
(78) Konsolakis, M.; Yentekakis, I. V.; Pekridis, G.; Kaklidis, N.; Psarras, A. C.; Marnellos, G. E. *Appl. Catal., B* **2013**, *138*, 191−198.
(79) Jones, I. Z.; Bennett, R. A.; Bowker, M. *Surf. Sci.* **1999**, *439*, 235−248.
(80) Gabasch, H.; Knop-Gericke, A.; Schloegl, R.; Borasio, M.; Weilach, C.; Rupprechter, G.; Penner, S.; Jenewein, B.; Hayek, K.; Kloetzer, B. *Phys. Chem. Chem. Phys.* **2007**, *9*, 533−540.
(81) Campbell, C. T.; Ertl, G.; Kuipers, H.; Segner, J. A. *Surf. Sci.* **1981**, *107*, 220−236.
(82) Guo, X.; Hoffman, A.; Yates, J. T., Jr. *J. Chem. Phys.* **1989**, *90*, 5787−5792.
(83) Leisenberger, F. P.; Koller, G.; Sock, M.; Surnev, S.; Ramsey, M. G.; Netzer, F. P.; Klötzer, B.; Hayek, K. *Surf. Sci.* **2000**, *445*, 380−393.
(84) Campbell, C. T. *Phys. Rev. Lett.* **2006**, *96*, 066106.
(85) Castellazzi, P.; Groppi, G.; Forzatti, P. *Appl. Catal., B* **2010**, *95*, 303−311.